

Aqueous Colloidal Mesoporous Nanoparticles with Ethenylene-Bridged Silsesquioxane Frameworks

Chihiro Urata,[†] Hironori Yamada,[†] Ryutaro Wakabayashi,^{†,‡} Yuko Aoyama,[†] Shota Hirosawa,[§] Satoshi Arai,^{||} Shinji Takeoka,^{*,§} Yusuke Yamauchi,^{⊥,‡} and Kazuyuki Kuroda^{*,†,‡}

[†]Department of Applied Chemistry, Faculty of Science and Engineering, Waseda University, Japan

[‡]Kagami Memorial Research Institute for Material Science and Technology, Waseda University, Japan

[§]Department of Life Science and Medical Bioscience, Faculty of Science and Engineering, Waseda University, Japan

^{||}Comprehensive Research Organization, Waseda University, Tokyo, Japan

[⊥]World Premier International (WPI) Research Center, International Center for Materials Nanoarchitectonics (MANA), National Institute for Materials Science (NIMS), Japan

^{*}Precursory Research for Embryonic Science and Technology (PRESTO), Japan Science and Technology Agency (JST), Japan

S Supporting Information

ABSTRACT: Aqueous colloidal mesoporous nanoparticles with ethenylene-bridged silsesquioxane frameworks with a uniform diameter of ~20 nm were prepared from bis-(triethoxysilyl)ethenylene in a basic aqueous solution containing cationic surfactants. The nanoparticles, which had higher hydrolysis resistance under aqueous conditions, showed lower hemolytic activity toward bovine red blood cells than colloidal mesoporous silica nanoparticles.

Aqueous colloidal solutions containing dispersed nanomaterials less than 100 nm in size have received much attention in practical fields, such as in biomedical, catalytic, and coating applications, because of the transparency of the solutions, the diffusivity and mobility of the nanoparticles, and the lower toxicity of aqueous systems.¹ Among nanomaterials, mesoporous nanoparticles have unique features.² Internal mesopores within nanoparticles can be used in various ways, including storage of large biomolecules, reactions in confined spaces, and communications between functional groups inside and outside the nanoparticles while retaining the colloidal state. Previous studies on colloidal mesoporous silica nanoparticles have shown their potential uses as drug carriers and biosensors.² However, silica frameworks present drawbacks for applications. For example, they show moderately low chemical stability under aqueous and humid circumstances.³ In addition, it is well-known that silanol induces the hemolysis of red blood cells (RBCs).⁴ To date, studies aimed at overcoming the drawbacks of silica frameworks have attempted to use organofunctionalization.⁵ However, an inhomogeneous distribution of organic groups on the mesopore surfaces and unwanted reactions of modifiers are unavoidable.⁶ Therefore, increasing the ability of the frameworks of colloidal mesoporous nanoparticles to be used without modification is highly demanded.

To circumvent the problem of the use of silica, bridged silsesquioxanes are some of the best candidates, as they have a variety of interesting features.⁷ A number of mesoporous silsesquioxane materials with several organic bridging groups, such as

aliphatic, aromatic, and metal complexes, have been synthesized as powders, films, and monoliths and demonstrated interesting properties for optical, electric, and catalytic applications.^{6,8} Although many reports have focused on the functions of organic bridging groups, the interesting features of silsesquioxane frameworks are not limited to these functions. They also exhibit both higher stabilities of the bonds⁶ in silsesquioxanes and the tuned acidities of silanol groups.⁹ Therefore, colloidal mesoporous nanoparticles with silsesquioxane frameworks are expected to show much higher stability against water and lower hemolysis activity than colloidal mesoporous silica nanoparticles.

Although the preparation of nanoparticles with silsesquioxane frameworks has been reported,¹⁰ the simultaneous achievement of dispersity, mesoporosity, and downsizing (to less than ~100 nm in particle size) of silsesquioxane nanoparticles has not been reported to date. In the case of bridged-type alkoxysilanes, the bulkiness and chemical characters of the bridging groups greatly affect the sol–gel reaction and the surface properties, which make the realization of colloidal nanoparticles difficult. This study discloses the preparation of such nanoparticles for the first time.

Here we report a facile route for preparing aqueous dispersed colloidal mesoporous nanoparticles with ethenylene-bridged silsesquioxane frameworks (CMP-SQ), the diameter of which is uniformly ~20 nm, by using bis-(triethoxysilyl)ethenylene (BTEE) as a framework source. CMP-SQ was prepared according to our previous report^{11a} using a newly developed two-step process involving preparation of dispersed mesostructured nanoparticles and subsequent dialysis. At first, colloidal mesostructured nanoparticles were prepared in a weakly basic solution containing hexadecyltrimethylammonium bromide (C₁₆TMABr) by adding BTEE. The molar ratio of the precursor solution was Si: C₁₆TMABr:TEA:H₂O = 1:0.50:0.25:1200. Next, the colloid was transferred into a dialysis membrane and dialyzed to remove C₁₆TMABr. To verify the effectiveness of the frameworks relative to silica, a degradation test in phosphate-buffered saline (PBS, pH 7.4) and an RBC hemolysis test were performed. For control experiments, colloidal silica (CS) nanoparticles and

Received: February 26, 2011

Published: May 03, 2011

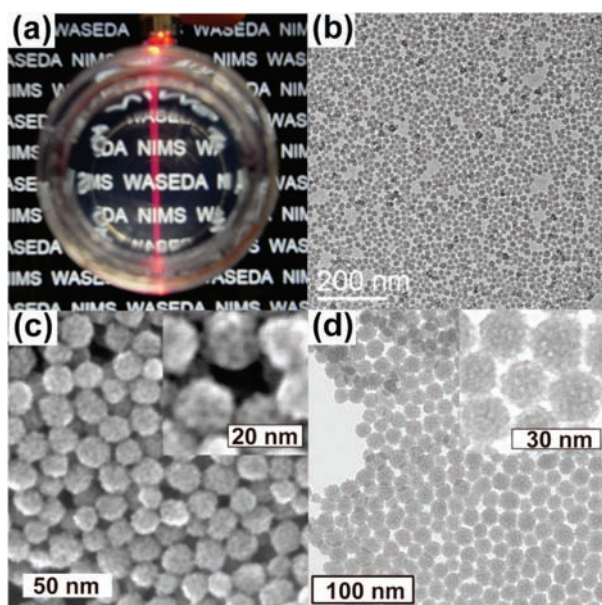


Figure 1. (a) Appearance of CMP-SQ (0.25 wt %). (b) Transmission electron microscopy (TEM) image of CMP-SQ. (c) Scanning electron microscopy (SEM) image of CMP-SQ. (d) Bright-field scanning TEM (STEM) image of CMP-SQ.

colloidal mesoporous silica nanoparticles (CMP-Si)¹¹ with diameters of ~ 20 nm were prepared as a typical example (see the Supporting Information for the detailed experimental conditions).

As shown in Figure 1a, CMP-SQ was almost transparent, with a clear Tyndall light scattering of the colloidal solution (0.25 wt %). The UV–vis transmittance spectrum of CMP-SQ (Figure S1b in the Supporting Information) shows transparency in the visible-light region. The UV–vis absorbance spectrum (Figure S1c) shows the presence of an absorption band at wavelengths less than 250 nm, which is assignable to the ethynylene group. In contrast, the band was not detected for a filtrate of CMP-SQ, which was separated with a centrifugal filter device (see the Supporting Information). Consequently, the UV–vis data indicate the presence of well-dispersed nanoparticles in the solution. The dispersity of the colloid was further confirmed by dynamic light scattering, which revealed a mean diameter of 24 nm. The colloid could be concentrated up to 26 wt % while retaining the transparency (Figure S1a). In addition, the aggregation of nanoparticles was not observed after repeated concentration–dilution cycles (10 times) at 2 and 20 wt % (Figure S2). The isoelectric point (IEP) of CMP-SQ was estimated to be between 5 and 6 from the ζ -potential data for CMP-SQ (Figure S3). The higher IEP of CMP-SQ in comparison with a silica surface (~ 2) can be explained by the reduction of the silanol acidity induced by an electron-donating ethynylene bridging group.⁹

Electron microscopy images revealed the presence of uniform nanoparticles with diameters of ~ 20 nm (Figure 1b–d) and black and white contrast within each nanoparticle (insets of Figure 1c,d). The presence of the mesostructure was also confirmed for a dried sample by the powder X-ray diffraction pattern, which contained a broad peak at 2.4° ($d = 4.6$ nm) (Figure S4a). The pattern was similar to that of aggregated mesoporous nanoparticles reported by Haskouri et al.^{10c} The surface area and pore volume of dried CMP-SQ (d-CMP-SQ)

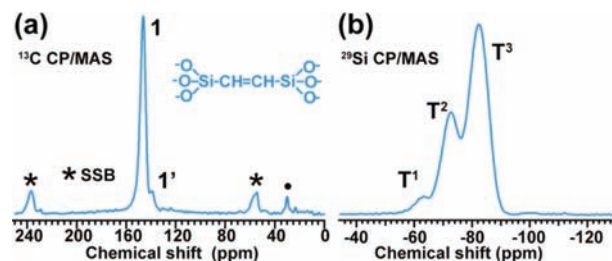


Figure 2. Solid-state CP/MAS NMR spectra of d-CMP-SQ: (a) ^{13}C (● indicates the residual C_{16}TMA); (b) ^{29}Si .

were calculated to be $640 \text{ m}^2/\text{g}$ and $0.57 \text{ cm}^3/\text{g}$, respectively (Figure S4b). The pore size distribution obtained using the nonlocal density functional theory (NLDFT) method showed two broad peaks in the mesopore range (Figure S4c). Thermogravimetric analysis (Figure S5) suggested that the removal of C_{16}TMA was almost complete ($>99\%$). The ^{13}C cross-polarization/magic-angle-spinning (CP/MAS) NMR spectrum of d-CMP-SQ showed the presence of ethynylene units by signals at 139 ppm ($1'$, cis isomer) and 146 ppm (1 , trans isomer)^{7,12} (Figure 2). The ^{29}Si CP/MAS NMR spectrum of d-CMP-SQ showed only three signals at -82.3 , -72.5 , and -63.3 ppm, which were assignable to T^3 , T^2 , and T^1 units [$\text{T}^x = \text{RSi}(\text{OH})_{3-x}(\text{OSi})_x$], respectively, indicating the formation of the silsesquioxane frameworks.

We tried to prepare several colloidal mesoporous silsesquioxane nanoparticles with methylene-, ethylene-, ethynylene-, and phenylene-bridged bis(triethoxysilane)s under the same conditions as CMP-SQ. Every silsesquioxane precursor, except for one containing a phenylene group, led to the formation of colloidal nanoparticles with a mesostructure (their appearances and TEM images are shown in Figure S6). For silsesquioxanes with larger bridging groups, such as phenylene, the hydrophobicity of the monomeric species may inhibit dispersion in water. Therefore, the compactness of the bridging groups is important for realizing the colloidal mesoporous nanoparticles.

To verify the effectiveness of the silsesquioxane frameworks with respect to degradation resistance toward phosphate-buffered saline (PBS), dialysis tubes including CMP-Si or CMP-SQ were immersed in the solution. As shown in Figure 3a, $\sim 18\%$ of the CMP-Si framework was dissolved after 25 h of immersion. In contrast, only $<1\%$ of the CMP-SQ framework was dissolved. In the investigation of the degradation for 15 days (Figure 3b), 90% of the CMP-Si degraded within 10 days. On the contrary, only $<2\%$ of CMP-SQ was degraded even after 15 days. Obviously, the resistance of the ethynylene-bridged silsesquioxane framework toward hydrolysis in a PBS solution is higher, and this is a result of the greater stability of the bonds in a silsesquioxane framework. This stability is expected to be suitable for long-term bioimaging. For use of such nanoparticles as a drug carrier, decomposition after the release of the drug should be considered. Stimuli-responsive units and/or biodegradable groups can be incorporated into the frameworks for these purposes.

Figure 4 shows the hemolysis behavior of three types colloidal nanoparticles (CMP-SQ, CMP-Si, and CS) in PBS solution (pH 7.4) (TEM images of CMP-Si and CS are shown in Figure S7). The hemolytic activity was found to be ordered as follows; $\text{CS} \gg \text{CMP-Si} > \text{CMP-SQ}$. Although the detailed mechanism of hemolysis of RBCs by silica is not well understood, it has been suggested that the hemolytic activity of silica is related to the density of surface silanol groups.⁴ In particular,

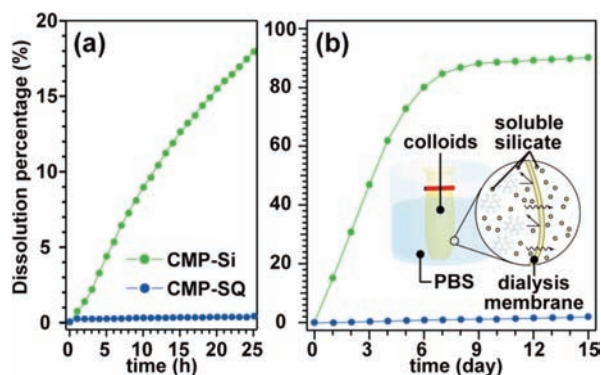


Figure 3. Dissolution behavior of CMP-Si and CMP-SQ in a PBS solution for (a) 25 h and (b) 15 days. The inset in (b) illustrates the scheme of this experiment. CMP-SQ was aggregated in the solution after 24 h.

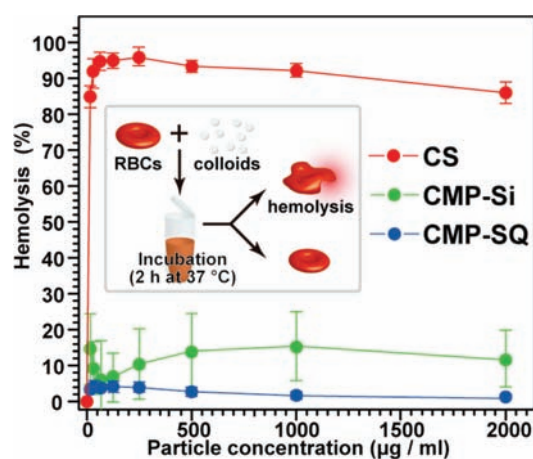


Figure 4. Percentage of hemolysis of RBCs in the presence of three kinds of nanoparticles at different concentrations ranging from 10 to 2000 $\mu\text{g}/\text{mL}$. The inset shows a schematic of this experiment. Each data point represents the mean \pm standard deviation of three independent experiments ($n = 3$).

the electrostatic interaction between a negatively charged silica surface (silanolate group) and a positively charged trimethylammonium head groups of the membrane lipid, such as phosphatidylcholine and sphingomyelin, is considered to be crucial to the hemolytic behavior.^{4e}

As demonstrated by Slowing et al.,^{4e} the lower hemolytic activity of CMP-Si relative to CS in this experiment can be explained by the decrease of the silanol density by the presence of mesopores. The lower hemolytic activity of CMP-SQ relative to CMP-Si is considered to be a combination of the lower density and lower acidity of the silanol groups, which probably reduces the number of silanolate groups on the surface of the nanoparticles. Therefore, the introduction of silsesquioxane frameworks into colloidal porous nanoparticles is effective in reducing the hemolytic activity without any further modifications such as PEGylation. A toxicity study using standard cell lines, which will be useful in evaluating CMP-SQ as a biocompatible material, is under investigation.

In conclusion, aqueous dispersed colloidal mesoporous nanoparticles containing ethylene-bridged silsesquioxane frameworks and having a uniform diameter of ~ 20 nm were successfully obtained. We found that the nanoparticles, which had

higher hydrolysis resistance under aqueous conditions, showed lower hemolytic activity toward bovine red blood cells than did colloidal mesoporous silica nanoparticles, presumably because of the longer Si–Si distance and lower acidity of the silanol group. This report has demonstrated not only the possibility of preparing colloidal nanoparticles apart from silica but also the usefulness of silsesquioxane frameworks without any further modifications. We believe that the degradation behavior and biocompatibility of the nanoparticles will be optimally tuned for biological applications by the design of the bridging groups. It has recently been reported that nanoparticles with sizes of <20 nm can pass through the blood brain barrier,¹³ blood vessel walls, and the gastrointestinal epithelium, which will be useful for cancer therapies.¹⁴ These colloidal porous nanoparticles are promising for various biotechnological applications, such as drug carriers as well as biosensors, artificial bionanoparticles, and hemocompatible coatings.

■ ASSOCIATED CONTENT

S Supporting Information. Materials, detailed experimental conditions, and characterizations. This material is available free of charge via the Internet at <http://pubs.acs.org>.

■ AUTHOR INFORMATION

Corresponding Author

kuroda@waseda.jp; takeoka@waseda.jp

■ ACKNOWLEDGMENT

The authors express their appreciation to Mr. M. Fuziwaru (Waseda University) for the TEM observations. The present study was supported by the Global COE Program “Practical Chemical Wisdom” and the Elements Science and Technology Project “Function Design by Precision Synthesis of Silicon–Oxygen Based Materials” from the Ministry of Education, Culture, Sports, Science, and Technology (MEXT). C.U. received financial support in the form of a grant-in-aid from the Japan Society for Promotion of Science Fellows.

■ REFERENCES

- (1) (a) Harada, A.; Kataoka, K. *Prog. Polym. Sci.* **2006**, *31*, 949–982. (b) Pellegrino, T.; Kudera, S.; Liedl, T.; Muñoz, J.; Manna, L.; Parak, W. J. *Small* **2005**, *1*, 48–63. (c) Wang, P. *Curr. Opin. Biotechnol.* **2006**, *17*, 574–579. (d) Goesmann, H.; Feldmann, C. *Angew. Chem., Int. Ed.* **2010**, *49*, 1362–1395. (e) Kotov, N. A. *Science* **2010**, *330*, 188–189.
- (2) (a) Coti, K. K.; Belowich, M. E.; Liong, M.; Ambrogio, M. W.; Lau, Y. A.; Khatib, H. A.; Zink, J. I.; Khashab, N. M.; Stoddart, J. F. *Nanoscale* **2009**, *1*, 16–39. (b) Lee, C.-H.; Lin, T.-S.; Mou, C.-Y. *Nano Today* **2009**, *4*, 165–179. (c) Klichko, Y.; Liong, M.; Choi, E.; Angelos, S.; Nel, A. E.; Stoddart, J. F.; Tamanoi, F.; Zink, J. I. *J. Am. Ceram. Soc.* **2009**, *92* (Suppl. s1), S2–S10. (d) Wang, Y.; Price, A. D.; Caruso, F. *J. Mater. Chem.* **2009**, *19*, 6451–6464. (e) Rosenholm, J. M.; Sahlgren, C.; Lindén, M. *Nanoscale* **2010**, *2*, 1870–1883. (f) Vivero-Escoto, J. L.; Slowing, I. I.; Trewyn, B. G.; Lin, V. S.-Y. *Small* **2010**, *6*, 1952–1967.
- (3) (a) He, Q.; Shi, J.; Zhu, M.; Chen, F. *Microporous Mesoporous Mater.* **2010**, *131*, 314–320. (b) Cauda, V.; Schlossbauer, A.; Bein, T. *Microporous Mesoporous Mater.* **2010**, *132*, 60–71. (c) Izquiero-Barba, I.; Colilla, M.; Manzano, M.; Vallet-Regí, M. *Microporous Mesoporous Mater.* **2010**, *132*, 442–452. (d) Hoshikawa, Y.; Yabe, H.; Nomura, A.; Yamaki, T.; Shimojima, A.; Okubo, T. *Chem. Mater.* **2010**, *22*, 12–14.
- (4) (a) Nash, T.; Allison, A. C.; Harington, J. S. *Nature* **1966**, *210*, 259–261. (b) Gerashchenko, B. I.; Gun'ko, V. M.; Gerashchenko,

I. I.; Mironyuk, I. F.; Lebeda, R.; Hosoya, H. *Cytometry* **2002**, *49*, 56–61. (c) Hadnagy, W.; Marssets, B.; Idel, H. *Int. J. Hyg. Environ. Health* **2003**, *206*, 103–107. (d) Murashov, V.; Harper, M.; Demchuk, E. *J. Occup. Environ. Hyg.* **2006**, *3*, 718–723. (e) Slowing, I. I.; Wu, C.-W.; Vivero-Escoto, J. L.; Lin, V. S.-Y. *Small* **2009**, *5*, 57–62. (f) Lin, Y.-S.; Haynes, C. L. *J. Am. Chem. Soc.* **2010**, *132*, 4834–4842.

(5) (a) Lin, Y.-S.; Haynes, C. L. *Chem. Mater.* **2009**, *21*, 3979–3986. (b) Cauda, V.; Schlossbauer, A.; Bein, T. *Microporous Mesoporous Mater.* **2010**, *132*, 60–71. (c) Lin, Y.-S.; Abadeer, N.; Haynes, C. L. *Chem. Commun.* **2011**, *47*, 532–534. (d) Suteewong, T.; Sai, H.; Cohen, R.; Wang, S.; Bradbury, M.; Baird, B.; Gruner, S. M.; Wiesner, U. *J. Am. Chem. Soc.* **2011**, *133*, 172–175.

(6) (a) Hoffmann, F.; Cornelius, M.; Morell, J.; Fröba, M. *Angew. Chem., Int. Ed.* **2006**, *45*, 3216–3251. (b) Fujita, S.; Inagaki, S. *Chem. Mater.* **2008**, *20*, 891–908.

(7) Loy, D. A.; Shea, K. J. *Chem. Rev.* **1995**, *95*, 1431–1442.

(8) (a) Ro, H. W.; Char, K.; Jeon, E.-C.; Kim, H.-J.; Kwon, D.; Lee, H.-J.; Lee, J.-K.; Rhee, H.-W.; Soles, C. L.; Yoon, D. Y. *Adv. Mater.* **2007**, *19*, 705–710. (b) Ro, H. W.; Popova, V.; Chen, L.; Forster, A. M.; Ding, Y.; Alvine, K. J.; Krug, D. J.; Laine, R. M.; Soles, C. L. *Adv. Mater.* **2011**, *23*, 414–420.

(9) Brinker, C. J.; Scherer, G. W. *Sol–Gel Science: The Physics and Chemistry of Sol–Gel Processing*; Academic Press: San Diego, CA, 1990; pp 142–143.

(10) (a) Cho, E.-B.; Kim, D.; Jaroniec, M. *Microporous Mesoporous Mater.* **2009**, *120*, 252–256. (b) Du, H.; Hamilton, P. D.; Reilly, M. A.; d'Avignon, A.; Biswas, P.; Ravi, N. *J. Colloid Interface Sci.* **2009**, *340*, 202–208. (c) Haskouri, J. E.; Zárata, D. Q.; Guillem, C.; Beltrán-Porter, A.; Caldés, M.; Marcos, M. D.; Beltrán-Porter, D.; Latorre, J.; Amorós, P. *Chem. Mater.* **2002**, *14*, 4502–4504.

(11) (a) Urata, C.; Yamauchi, Y.; Aoyama, Y.; Imasu, J.; Todoroki, S.; Sakka, Y.; Inoue, S.; Kuroda, K. *J. Nanosci. Nanotechnol.* **2008**, *8*, 3101–3105. (b) Urata, C.; Aoyama, Y.; Tonegawa, A.; Yamauchi, Y.; Kuroda, K. *Chem. Commun.* **2009**, 5094–5096.

(12) (a) Loy, D. A.; Carpenter, J. P.; Yamanaka, S. A.; McClain, M. D.; Greaves, J.; Hobson, S.; Shea, K. J. *Chem. Mater.* **1998**, *10*, 4129–4140. (b) Vercaemst, C.; Ide, M.; Wiper, P. V.; Jones, J. T. A.; Khimyak, Y. Z.; Verpoort, F.; Voort, P. V. D. *Chem. Mater.* **2009**, *21*, 5792–5800.

(13) Sonavane, G.; Tomoda, K.; Makino, K. *Colloids Surf., B* **2008**, *66*, 274–280.

(14) (a) Jong, W. H. D.; Borm, P. J. A. *Int. J. Nanomed.* **2008**, *3*, 133–149. (b) Wang, X.; Yang, L.; Chen, Z.; Shin, D. M. *Ca-Cancer J. Clin.* **2008**, *58*, 97–110.